ChemComm

Accepted Manuscript

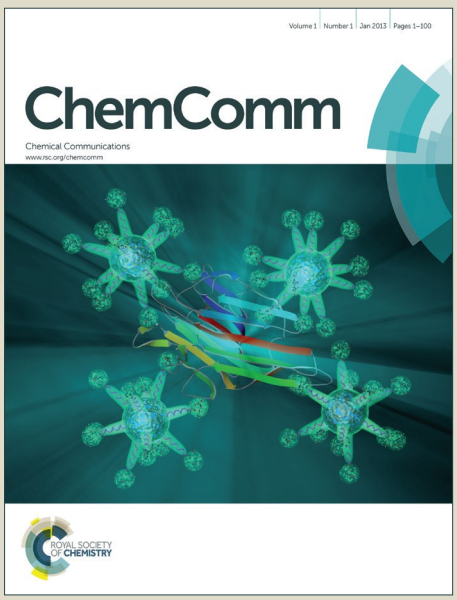

ROYAL SOCIETY OF CHEMISTRY

www.rsc.org/chemcomm

COMMUNICATION

Total chemical synthesis of a polymer/graphene nanocomposite

Received 00th January 20xx,
Accepted 00th January 20xx

DOI: 10.1039/x0xx00000x

www.rsc.org/

Rodrigo V. Salvatierra,[a] Carlos E. Cava,[b] Lucimara S. Roman,[b] Marcela M. Oliveira[c] and Aldo J.G. Zarbin[a*]

A versatile and room temperature synthesis of thin films of polymer/graphene is reported. Drastically differing from other methods, not only the polymer but also the graphene are completely build from their simplest monomers (thiophene and benzene) in a one-pot polymerization reaction at a liquid-interface. Materials were characterized and electronic properties are presented.

Nanocomposites between different categories of polymers and carbon nanostructures (carbon nanotubes or graphene) are in the center of the most recent materials development.[1] Several synthetic procedures and approaches have been developed to prepare that fascinating class of material, as for example a mechanical mixture of the components, a mixture of dispersions of either components, or the in situ polymerization over the carbon nanostructures.[2-3] For all known routes to carbon nanostructures-based polymeric nanocomposites, there are different ways to prepare the polymer, but the carbon nanostructure should necessarily be pre-prepared and mixed during the preparative steps.

In which concerns the structure and morphology of these nanocomposites, it is desirable that the carbon nanomaterial stays homogeneously distributed over the polymer, enhancing the contact area between the two components, an important factor responsible for the observable properties.[2,3] The processability of these materials is as important as their preparation, because the way in which the material will be presented (for example as a monolith, self-standing film or thin film) will determine the range of possible applications for it.[1] So, it is very common to find materials presenting unique properties that will not result in real application, due to their unprocessability. The class of polythiophenes (PTs) represents an emblematic example of this situation. PTs have some unique properties that are closely related to their great scientific and technological interest.[4,5] For example, the unsubstituted PT is expected to provide excellent performance as active layer in organic solar cells,[6-7] because of the close contact of the polymeric chains (which improves the charge transport) and the excellent stability in air (soluble polyalkylthiophenes are air sensitive).[4,8] However, this application requires the preparation of PT as thin films which is challenging due to the insolubility of PT, as pointed out by sparse works dedicated to the thin film production of PT.[9-11]

Recently, we reported that liquid-liquid interfacial systems can be an interesting confined medium in which unprocessable materials can be assembled as a thin and transparent films, easily transferable to ordinary substrates, enabling its study in thin film based devices.[12-15] We applied this system for self-assembling thin films of polyaniline with carbon nanotubes and graphene. Otherwise we also reported that the same liquid-liquid interface between water and benzene can lead to the synthesis of large graphene structures, based on a polymerization of benzene by $FeCl_3$ and subsequent coupling reactions with benzene mediated by the water/oil interface.[16] This reaction is based on an extensive work of Kovacic *et al* about the poly-(p-phenylene) (PPP) reactions,[17-22] and it is fundamentally different from other reports about the chemical synthesis of graphene involving specialized phenylene molecules,[23-25] and other most recent approaches.[26-27]

Therefore, based on these two possible outcomes from the liquid-liquid interface, we report here the synthesis of a nanocomposite in which both phases (polymer and carbon nanomaterial) are chemically synthesized in one-step and one-pot reaction, starting from their simplest monomers (thiophene and benzene), giving rise to a polythiophene/graphene material. The graphene phase is equally distributed over the PT and the whole material is already synthesized/processed as a thin and transparent film assembled at the liquid-liquid interface. A spectroscopic characterization of the polymer/graphene structure is provided. The electronic properties were evaluated in terms of charge carriers mobility and enhanced photovoltaic properties caused by the presence of graphene in the polythiophene thin films. As far as we know, this is the first report on a nanocomposite synthesis in which both materials are simultaneously synthesized. Additionally, this is the first report of the chemical synthesis of unsubstituted PT directly as a thin film (neat or in hybrid films).

The Figure 1a presents the general scheme for preparation of polythiophene/graphene thin films. First, a dispersion of anhydrous $FeCl_3$ in benzene is prepared by sonication (see Supplem. Info, Exp. Section.) and then added to an emulsion formed by water and thiophene. Since two reactions took place simultaneously in this system, we shall describe what happen at the interface separately. In which concerns the PT synthesis, when the two phases are in contact, the insoluble $FeCl_3$ spontaneously migrates to the aqueous phase and the thiophene migrate to the organic phase. So, both of these reactants come into contact exactly at the interface, producing PT in a reaction according to Fig. 1a, creating a red film that behaves as a transparent and malleable "skin" assembled at the liquid-liquid interface (Fig. 1d). The $FeCl_3$ dispersion in benzene is necessary since the chemical polymerization of thiophene requires anhydrous $FeCl_3$,[28] opposite to our previous synthesis protocol of polyaniline films (monomer in organic phase, oxidant in water).[12-15] The same synthesis can be performed in non-aromatic solvents like chloroform (sample PT-chloroform) and hexane (sample PT-hexane), producing PT but without the presence of graphene.

[a] Department of Chemistry, Federal University of Paraná (UFPR), Centro Politecnico, CP 19032, CEP 81531-980, Curitiba-PR-Brazil, aldozarbin@ufpr.br
[b] Department of Physics, Federal University of Paraná (UFPR), Curitiba-PR-Brazil.
[c] Department of Chemistry and Biology, Federal Technological Univertsity of Paraná (UTFPR), Curitiba-PR-Brazil.

† Electronic Supplementary Information (ESI) available: Experimental details, [details of any supplementary information available should be included here]. See DOI: 10.1039/x0xx00000x

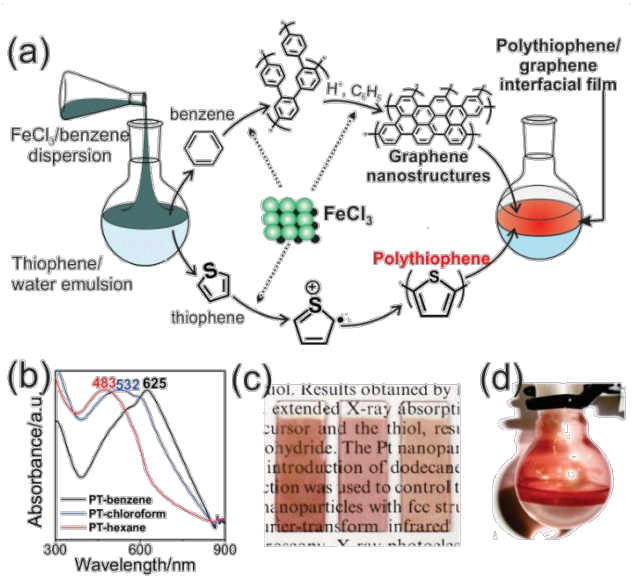

Figure 1. (a) Scheme of polymer/grapheme synthesis starting from benzene and thiophene using the liquid-liquid interfacial system; (b) UV-Vis spectrum of PT films; (c) photographs of PT interfacial thin films deposited over glass slides (from left to right, PT-benzene, PT-chloroform, PT-hexane); (d) photograph of PT interfacial thin film in a flask with liquid-liquid system.

The red colour of the PT films (Fig. 1c) indicates the neutral state (undoped), as observed by the 500-600 nm absorption band in UV-Vis spectra (Fig.1b). The PT produced with benzene presents the most red-shifted absorption band which is related to a more conjugated structure,[4] caused by the presence of graphene. The interfacial films can be easily removed from the interface, as well their thicknesses controlled by the synthesis parameters (Supplem. Info, Fig. **S1** and **S2**).

Analyzing the same interfacial system but now for the graphene synthesis, we observed previously that the dispersion of $FeCl_3$ and benzene prepared by sonication can lead to the formation of small oligophenylens/polyphenylenes, resulting from the benzene polymerization.[18-20] When this whole dispersion containing oligophenylenes, large excess of benzene and $FeCl_3$ found water in the interfacial system, new coupling reactions (incorporation of new benzene monomers to the pre-made oligophenylene) take place, now catalyzed by transient acid species created at the fast contact of the excess of $FeCl_3$ and the water phase (interface mediated reaction), a mechanism known as Scholl reaction.[21,22,29] We recently demonstrate that controlling this whole process these reactions can produce graphene.[16] It is important to point out that our strategy is similar to the extensive work of Kovacic, differing from other more sophisticated methods to chemically synthesize graphene.[23-27]

Vibrational spectroscopy was used to gain insight on the chemical structures of the films. Raman (514.5 nm) and infrared (IR) spectra are presented in Figure 2, confirming the occurrence of unsubstituted polythiophene (Fig. 2a-c). The sp^2 structure of the pure graphene sample is evidenced by the Raman spectrum in Figure 2d, featuring three main bands located around 1350, 1588 and 2700 cm^{-1}, assigned to the D, G and G' bands, a fingerprint of graphene and sp^2 carbon materials.[30] Due to the strong resonant effect of PT in Raman spectrum, we could not observe the graphene modes in the spectrum of PT-benzene (Fig. 2a), although its observation within the polymer is more straightforward using electron microscopy techniques as will be presented. Comparing the polythiophene spectrum of samples prepared with benzene, chloroform and hexane, we observe that the solvent has influence over the quality of the PT. It becomes evident that the samples prepared with hexane (Fig. 2c) are different from those prepared with benzene and chloroform, whose spectra (Raman and IR) are comparable (Fig. 2a-2b). Three main features confirms this: **(1)** the ratio of the symmetric (~1[illegible] cm^{-1}) to the antisymmetric (1490 cm^{-1}) (IR spectrum) stretchin[illegible] mode of $C_\alpha=C_\beta$ ($I_{sym,1439}/I_{asym,1490}$) is much higher for PT-hexan[illegible] indicating much lower conjugation lengths;[31,32] **(2)** the ratio of 701 cm^{-1} band (out-of-plane ring symmetric bending) in Raman spectrum over side bands (650, 681, 759 cm^{-1}) is much lower in PT-hexa[illegible] indicating more distorted PT chains;[31] **(3)** the ratio of 700/782 cm^{-1} band in IR spectrum (out-of-plane C-H bending in the [illegible]-monosubstituted and 2,5-disubstituted, respectively) is higher in PT-hexane, indicating lower degree of polymerization. This result indicates that the polythiophene produced in the samples PT-chloroform and PT-benzene are structurally comparable. The reason why the PT-hexane is structurally inferior to the other samples is related to the poor interaction of alkanes with $FeCl_3$, while chloroform and benzene are known to have strong interaction with Lewis acids.[17,19,33]

Transmission electron microscopy (TEM) images (Fig. 3) allow assessing more directly the presence of graphene in PT-benzene. The PT-hexane (Fig. 3e) presents the typical polymeric morphology characterized by fibrillar aggregates.[34] On the other hand, PT-benzene (Fig.3a-3d) shows regions in which the polymer fibers are observed mixed with graphene, as observed in Figure 3a-3c. The graphene structures are normally completely covered by fibers but they can be identified by the folded aspect of the sheets (Fig. 3c), as can be also seen in Figure 3f (pure graphene). Regions enriched with PT fibers can be also found, as in Figure 3d. The clear distinction of the graphene generated in PT-benzene sample can be evidenced in TEM by using also analytical techniques, like energy dispersive spectroscopy (EDS) and selected area electron diffraction (SAED) of PT-benzene to evaluate the crystalline character of the graphene. In the SAED (Fig. 3g), (corresponding to the area of Fig.3c) two sets of planes can be identified, corresponding to the plane (100) (inner circle) and (110) (outer circle) of graphene, proving its hexagonal lattice. Few hexagonal spot sets can be identified although the diffraction is the result of several small crystalline domains sheet giving the arc aspect.[35] The pure polymer SAED gives no diffraction pattern because of its amorphous nature. The intensity profile of SAED is provided in Fig. **S3** (corresponding to the dashed arrow in Fig. 3g) and provides the distance of the planes (100) and (110) (Fig. **S3**), corresponding to 2.12 Å and 1.25 Å, respectively, which is in close agreement with the values found for pure graphene (2.[illegible] and 1.22 Å).[35-36] In addition, EDS was obtained from the area of Figure 3c using scanning-transmission electron microscopy (STEM) mode

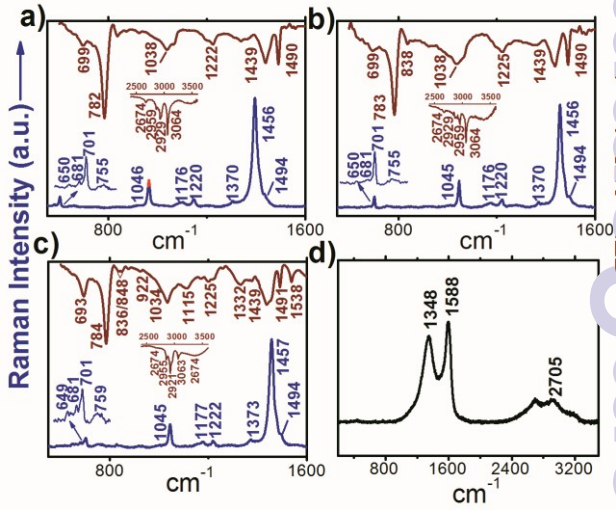

Figure 2. Normalized Raman and IR spectra (attenuated total reflectance - ATR) of th[illegible] PT films. (a) PT-Benzene; (b) PT-chloroform, (c) PT-hexane, (d) graphene (contr[illegible] experiment with benzene, without thiophene).

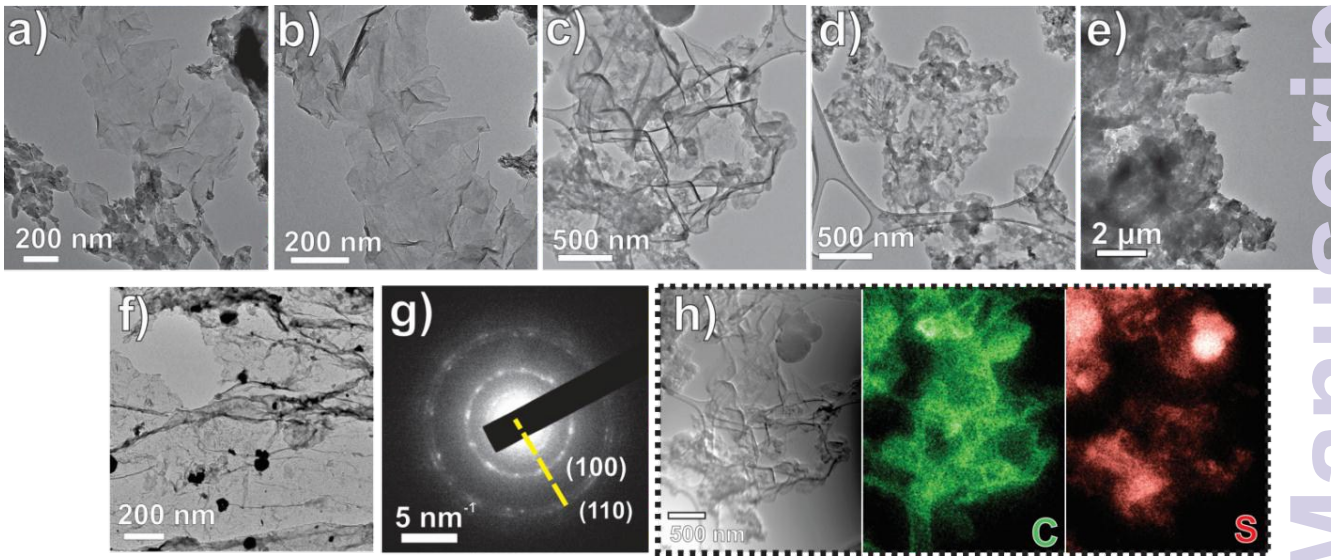

Figure 3. (a-d) Transmission electron microscopy (TEM) images of PT-benzene; (e) TEM image of PT-hexane; (f) TEM image of graphene sample; (g) selected area electron diffraction (SAED) of image presented in Fig. 3c. The profile of the dashed arrow is in Fig. S3; (h) STEM image of area in (c) and corresponding elemental maps of carbon and sulfur.

(Fig. **S4)**. The major signals in EDS spectrum are from carbon and sulfur, as expected by the presence of graphene and polythiophene fibers. The corresponding STEM image of Figure 3c is presented in Figure 3h along with the elemental mapping of carbon and sulfur. The carbon map clearly identifies the graphene sheets structure as well as the sulfur map identifies the polymer-rich areas. This data along with the proof of crystalline character provided by SAED (on the same area) confirm the distinct production of graphene sheets and polythiophene. It cannot be excluded that some thiophene units can be incorporated in the honeycomb structure of graphene during the interfacial polymerization, originating some pentagon rings along the graphene sheets.

The data presented and discussed till now evidences directly that the sample PT-benzene is a true nanocomposite between PT and graphene, both synthesized together in a one-pot reaction. To the best of our knowledge this is the first report on the preparation of a graphene-based polymeric nanocomposite in which both the components are chemically obtained from their molecular precursor. Cyclic voltammogram were performed to see the effect of graphene on the electrochemical properties of PT (Fig. 4). The PT samples present the typical oxidation potential (*p*-doping process) at 0.9 V. The well-known electrochromism of PT (Fig. 4c) was also observed and tested by UV-Vis spectro-electrochemistry. Spanning the potential range to -1 V (*vs* Ag/AgCl) (Fig. 4a) we observe a reversible processes only in PT-benzene, which is relative to the presence of graphene, since pure graphene sample also present activity in the same potential range (Fig. 4a). The reversible process at negative potentials can point out a higher electron affinity of graphene and, therefore, indicate that both process –*p* and *n* doping– can be separately operated in the PT-benzene as it is composed by two materials. On the other hand, the other PT samples show no reversible process at negative potential, as expected for pure PT.[37] In addition, we used the onset method to calculate the HOMO (highest occupied molecular orbital) and LUMO (lowest unoccupied molecular orbital) energies (data are displayed in Table **S1**). All the HOMO levels are in the range of ~5.5 eV, more negative than air oxidation threshold (~5.3 eV),[37] meaning that these films are completely air stable. The calculated band gaps also show lower values (~ 1.4 eV) for PT-benzene and PT-chloroform related to the PT-hexane (~1.8 eV), confirming the spectroscopic results.

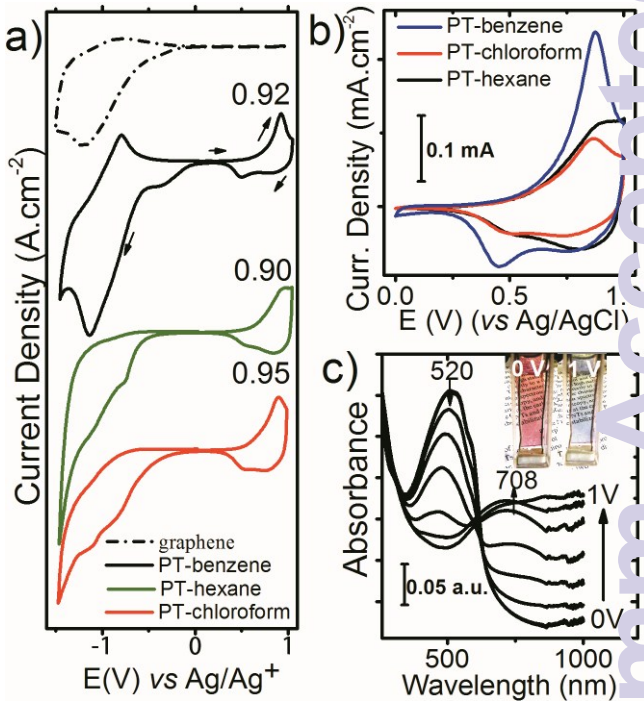

Figure 4. (a) Cyclic voltammograms of the films deposited over ITO (0.1 mol.L^{-1} $LiClO_4$ / CH_3CN, 20 mV.s^{-1}) Arrows indicate the scan direction, starting from 0.0 V; (b) CV in a smaller potential window; (c) UV-Vis spectroelectrochemistry of the PT-benzene at different applied potential (same experimental condition as described in (a)). The inset shows a picture of the film at 0.0 and 1.0 V of applied potential.

Finally, we characterize the electronic and light absorption properties of these PT-films and evaluate the effect of graphene on the PT properties. Current density (J) *vs* voltage (V) curves are presented in Figure 5b. We calculate the charge mobility of the PT films by fitting these curves using the space-charge limited current method (SCLC) (values and calculation are provided in Supplem. Info, Fig. **S5**).[38] We observed that PT-benzene has a higher mobility

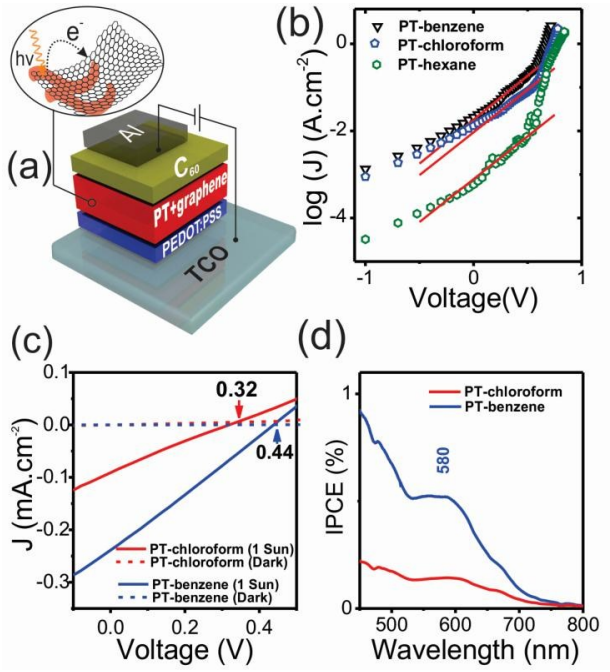

Figure 5. (a) Scheme of solar cell using PT-benzene or PT-chloroform as active layer; (b) current density (*J*) *vs* V curves for different films. Red lines correspond to SCLC fitting (see Supplem. Info, Fig. S5); (c) current density *vs* voltage of the solar cell under sun and dark and (d) Incident Photon-to-Current Efficiency (IPCE).

of 10^{-3} $cm^2.V^{-1}.s^{-1}$ (average value) related to the other PT-samples, significantly higher for an un-doped and completely air-stable PT thin film. The higher value compared to other samples is related to the presence of the graphene within the PT chains. Next, we evaluate the light absorption by constructing photovoltaic devices (Fig. 5a) using PT films as active layers. The J *vs* V curves in dark and light (Fig. 5c) show enhanced electrical current when PT-benzene is exposed to light, compared to the sample without graphene (PT-chloroform was chosen for control since it has similar PT structure as PT-benzene), improving the total device efficiency in four times ($\eta_{PT\text{-}benzene} = 2.7\times10^{-2}$ % efficiency compared to $\eta_{PT\text{-}chloroform} = 7\times10^{-3}$ %). (photovoltaic parameters in Suppl. Info, Table **S2**). This higher performance is credited to a more efficient exciton dissociation at the several interfaces created between graphene and polymer (inset Fig. 5a). This is further corroborated by the incident photon-to-current efficiency (IPCE) (Fig. 5d) which is higher for the PT-benzene. In addition, this data clarify that the photo-activity of the device comes from the polymer part of the nanocomposite, since the peak of activity (580 nm) matches with the visible absorption of PT (500 – 600 nm).

In conclusion, we presented here the first report on a synthesis of a graphene/polymer nanocomposites in which both phases are obtained together, processed as a thin film, in a simple and versatile one-pot reaction. Also, the work presents an innovative route to unsubstituted polythiophene thin films, which can be transferred to different kind of substrates. The presence of graphene improves and extends the properties of PT. In a general analysis, the results presented here can be extended to other systems where simultaneous chemical synthesis of graphene and a second material may be needed in order to obtain a highly interfaced hybrid material. This opens new possibilities in terms of material design and preparation compared to existing methods.

References

1 G. Ćirić-Marjanović, Synth. Met., 2013, **170**, 31
2 A. G. Macedo, C. F. N. Marchiori, I. R. Grova, L. Akcelrud, M. Koehler and L. S. Roman, *App. Phys. Lett*., 2011, **98**, 253501.
3 D. Fichou, ed., Handbook of oligo- and polythiophenes, Wiley-VCH, 1999
4 B. Arash, Q. Wang and V. K. Varadan, *Sci. Rep.*, 2014, **4**, 6479
5 R. D. McCullough, *Adv. Mater.*, 1998, **10**, 93
6 S. A. Gevorgyan and F. C. Krebs, Chem. Mater., 2008, **20**, 4386.
7 P. Kovacik, S. M. Willis, J. D. Matichak, H. E. Assender and A. A. R. Watt, Org. Electron., 2012, **13**, 687-696
8 X.-G. Li, J. Li, Q.-K. Meng and M.-R. Huang, *J. Phys. Chem.* B, 2009, **113**, 9718
9 L. M. H. Groenewoud, G. H. M. Engbers, J. G. A. Terlingen, H. Wormeester and J. Feijen, *Langmuir*, 2000, **16**, 6278
10 S. Nejati and K. K. S. Lau, *Langmuir*, 2011, **27**, 15223
11 S. Natarajan and S. H. Kim, *Chem. Commun*., 2006, 729
12 R. V. Salvatierra, M. M. Oliveira and A. J. G. Zarbin, *Chem. Mater*., 2010, **22**, 5222
13 S. H. Domingues, R. V. Salvatierra, M. M. Oliveira and A. J. G. Zarbin, *Chem. Commun*., 2011, **47**, 2592
14 R. V. Salvatierra, L. G. Moura, M. M. Oliveira, M. A. Pimenta and J. G. Zarbin, *J. Raman Spec*., 2012, **43**, 1094
15 R. V. Salvatierra, C. E. Cava, L. S. Roman and A. J. G. Zarbin, *Adv. Funct. Mater.*, 2013, **23**, 1490
16 R. V. Salvatierra, V. H. R. Souza, M. M. Oliveira and A. J. G. Zarbin, *Carbon*, 2015, **93**, 924
17 P. Kovacic and H. C. Volz, *J. Am. Chem. Soc*, 1959, **81**, 3261
18 P. Kovacic, C. Wu and R. W. Stewart, *J. Am. Chem. Soc*, 1960, **82**, 1917
19 P. Kovacic and C. Wu, *J. Pol. Sci*., 1960, **47**, 45
20 P. Kovacic and F. W. Koch, *J. Org. Chem*., 1963, **28**, 1864
21 P. Kovacic, F. W. Koch and C. E. Stephan, *J. Pol. Sci. Part A*, 1964, **2**, 1193
22 P. Kovacic and M. B. Jones, *Chem. Rev*., 1987, **87**, 357
23 M. Bieri, M. Treier, J. Cai, K. Ait-Mansour, P. Ruffieux, O. Groning, P. Groning, M. Kastler, R. Rieger, X. Feng, K. Mullen and R. Fasel, *Chem.Commun*. 2009, **45**, 6919
24 T. H. Vo, M. Shekhirev, D. A. Kunkel, M. D. Morton, E. Berglund, L. Kong, P. M. Wilson, P. A. Dowben, A. Enders, and A. Sinitskii, *Nat. Commun*., 2014, **5**, 3189
25 A. Narita, X. Feng, Y. Hernandez, S. A. Jensen, M. Bonn, H. Yang, I. A. Verzhbitskiy, C. Casiraghi, M. R. Hansen, A. H. R. Koch, G. Fytas, O. Ivasenko, B. Li, K. S. Mali, T. Balandina, S. Mahesh, S. De Feyter and K. Müllen, *Nat. Chem.*, 2014, **6**, 126
26 S. Y. Sawant, R. S. Somani, M. H. Cho, and H. C. Bajaj, *RSC Adv*., 2015, **5**, 46589
27 Y. Byun and A. Coskun, *Chem. Mater*., 2015, **27**, 2576
28 V. M. Niemi, P. Knuuttila, J.-E. Osterholm and J. Korvola, *Polymer*, 1992, **33**, 1559
29 M. Grzybowski, K. Skonieczny, H. Butenschön and D. T. Gryko, *Angew. Chem. Int. Ed*., 2013, **52**, 9900
30 A. Jorio, *ISRN Nanotechnology*, 2012, **2012**, 16
31 Y. Furukawa, M. Akimoto and I. Harada, *Synth. Met*., 1987, **18**, 15
32 M. Akimoto, Y. Furukawa, H. Takeuchi, I. Harada, Y. Soma and M. Soma, *Synth. Met*., 1986, **15**, 353
33 P. E. Hoggard, M. Gruber and A. Vogler, *Inorg. Chim. Acta*, 2003, **346**, 137
34 J. Huang and R. B. Kaner, *Chem. Commun*., 2006, **4**, 367
35 P. Y. Huang, C. S. Ruiz-Vargas, A. M. van der Zande, W. S. Whitney, M. P. Levendorf, J. W. Kevek, S. Garg, J. S. Alden, C. J. Hustedt, Y. Zhu, J. Park, P. L. McEuen and D. A. Muller, *Nature*, 2011, **469**, 38
36 Z. Czigány and L. Hultman, Ultramicroscopy, 2010, **110**, 815
37 D. M. de Leeuw, M. M. J. Simenon, A. R. Brown and R. E. F. Einerhand, *Synth. Met*., 1997, **87**, 53
38 A. Kokil, K. Yang and J. Kumar, *J. Pol. Sci. Pol. Phys*., 2012, **50**, 1130.